euronoise

Sound intensity variations in the presence of shallow-water internal waves passing through acoustic track

Jing Luo[a], Mohsen Badiey[a], Entin Karjadi[b], Boris Katsnelson[c], Alexander Tshoidze[c], James Moum[d] and James Lynch[e]

[a]University of Delaware, College of Marine and Earth Studies, S. College Street, Newark, DE 19716, USA
[b]College of Marine and Earth Studies, University of Delaware, Newark, DE 19716, USA
[c]Voronezh State University, 1, Universitetskaya sq., 394006 Voronezh, Russian Federation
[d]College of Oceanic and Atmospheric Sciences, Oregon State University, 104 COAS Administration Bldg, Corvallis, OR 93371, USA
[e]Woods Hole Oceanographic Institution, 98 Water Street, Bigelow 203A, MS-11, Woods Hole, MA 02543, USA
katz@phys.vsu.ru

Fluctuations of the low frequency sound field in the presence of an internal solitary wave (ISW) packet during the Shallow Water '06 (SW06) experiment are analyzed. Acoustic, environmental, and on-board ship radar image data were collected simultaneously before, during, and after a strong ISW packet passed through the acoustic track. Preliminary analysis of the acoustic wave temporal intensity fluctuations agrees with previously observed phenomena and the existing theory of the horizontal refraction mechanism, which causes fluctuations when the acoustic track is nearly parallel to the front of the internal waves.

1 Introduction

In shallow water regions, nonlinear internal solitary waves (ISW's) create an anisotropic water column that affects acoustic wave propagation. In recent years, experimental and modeling efforts [1-3] have been conducted to quantify acoustic wave interaction with ISW's. These studies suggest that there are three different mechanisms that can explain the intensity variations in the presence of ISW. The adiabatic regime corresponds to fluctuations of the sound field due to local variations of the water layer (i.e. sound speed and/or depth) at the position of the source or the receiver. Next, propagation can be dominated by the mode coupling regime, where the interaction with the internal waves can cause energy transfer between different modes which in turn can result in fluctuations in the intensity. Finally, there is the horizontal refraction regime in which the distribution of the acoustic field in the horizontal plane can cause fluctuations in the measured field. The last two situations can cause the more significant signal intensity fluctuations [1-3]. While the comparison of modeling results with data have previously shown the validity of this theory, a direct simultaneous measurement of the acoustic field and the ISW has not yet been reported to establish the transition among different mechanisms. In our previous work we separated propagation regimes depending on the angle between the ISW wave front and the direction of acoustic track. In SW06 experiment data studied in this paper, we present a data set where the acoustic track angle is kept unchanged while the internal wave slowly transects the acoustic track including the source-receiver geometry. When the ISW train is starting to cover the receiver array only and does not occupy all (or a significant part of) the acoustic track, we have the adiabatic regime. As the train moves and continues to cover the acoustic track, propagation changes to the horizontal refraction regime. Therefore, we have a direct transition between the two regimes.

The multi-institutional SW06 experiment was conducted on the New Jersey continental shelf from July to September 2006 at a location where internal wave activity has been observed and studied in the past[4]. In this paper, we focus on a particular internal wave event on August 17, 2006, for which a complete set of acoustic and environmental data were collected simultaneously. In addition, ISW surface signatures were captured continuously by the on-board radars of two research vessels prior to the arrival of and during the passing of the ISW packet over the acoustic track. The acoustic wave field variation is studied during this process. Other studies of the SW06 data in relation to the three dimensional modeling are being conducted separately [5,6].

2 Simultaneous acoustic and internal waves measurements

During SW06, both acoustic and environment data were collected simultaneously. In this paper we discuss the acoustic data from a particular acoustic source (NRL 300Hz) on the mooring denoted SW45. The source was located 72 m below the sea surface and 10.5 m above the sea floor at 39°10.957' N, 72°56.575' W, and transmitted 2.0489 second long Linear Frequency Modulating (LFM) signals between 270 and 330 Hz every 4 seconds (Fig. 1). This transmission continued for 7.5 minutes and then repeated every half hour. A vertical and horizontal receiver array (the "Shark VHLA") on mooring SW54 was located at 39°01.252' N, 73°02.983' W, about 20.2 km south of the NRL source. The vertical part of the receiver array consisted of 16 hydrophones with 3.5 m spacing and spanned from 13.5 m to 77.75 m below the surface. The horizontal part of the array consisted of 32 hydrophones on the seafloor with spacing of 15 m, providing 478 m of horizontal aperture. The sampling rate of the array was 9765.625 Hz. The acoustic track and the locations of the source and receiver are shown in Fig. 2. The water depth along the acoustic track was about 80 m.

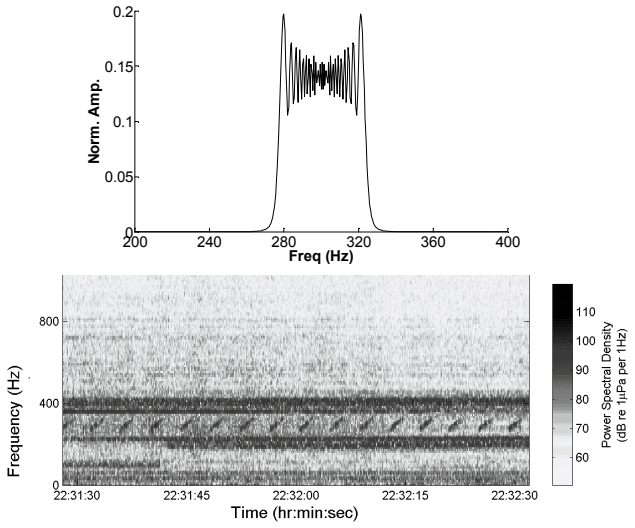

Fig. 1

On August 17, 2006, at about 18:00 GMT, the R/V Sharp from the University of Delaware was located at 38°59.262' N, 72°57.492' W and the R/V Oceanus from the Woods Hole Oceanographic Institution (WHOI) was located at 38°57.426' N, 72°56.676' W. They both observed the

origination of an ISW near the shelf break. This event was named Event 50 on R/V Sharp and Rosey on R/V Oceanus.

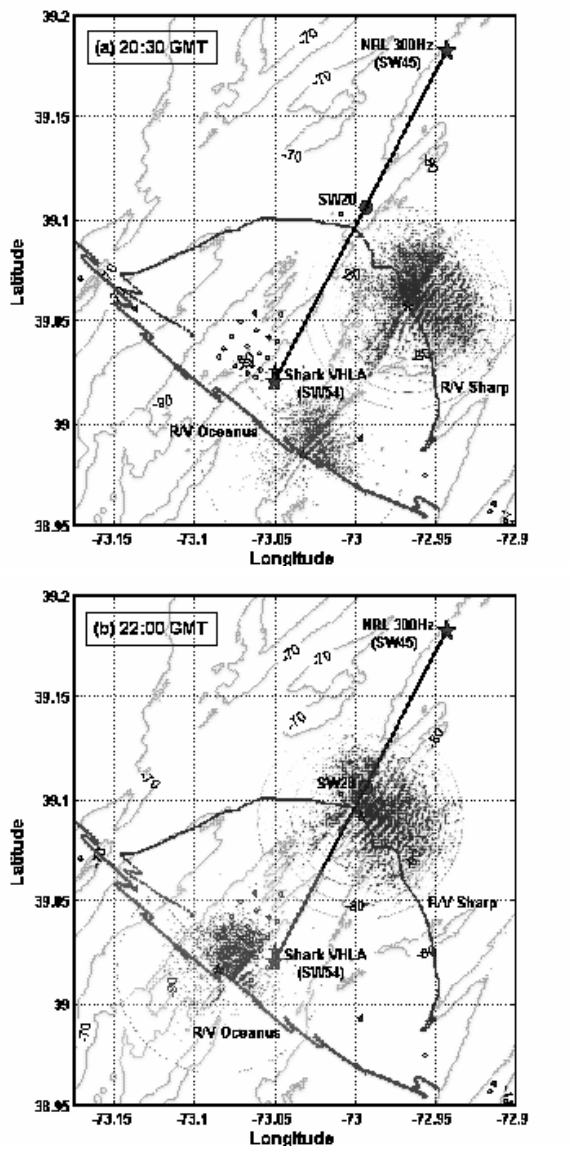

Fig. 2 Map of the experiment location showing the positions of the acoustic source (NRL 300 Hz on SW45 mooring), the receiver array (Shark VHLA on SW54 mooring) and a midpoint thermistor array (SW20) together with the two research vessels (R/V Sharp and R/V Oceanus) at two different geotimes. Times are (a) Tg_1 = 20:30 to 20:37:30 GMT, when the ISW has not reached the acoustic track, (b) Tg_2 = 22:00:00 to 22:07:30 GMT, when the ISW has occupied a large portion of the acoustic track including the receiver array. Ship tracks and radar images of R/V Sharp and R/V Oceanus are shown.

Fig.2 shows the track of each vessel following this event from 18:00 GMT on August 17 to 02:00 GMT on August 18, 2006. The R/V Sharp's track was semi circular, centered at the WHOI vertical and horizontal line array (Shark VHLA) with the ship being positioned on the trough of the leading ISW front and moving with the advancing front. The R/V Oceanus followed the same ISW packet from its initial location, while keeping a watch on the advancing wave front. Reversals in the track of R/V Oceanus indicate where the wave packet was crossed, and during these periods, intensive profiling of temperature, density, turbulence and velocities was conducted.

Both ships covered different parts of the ISW front, providing a large spatial coverage. The surface signatures of the ISW were recorded by on-board ship radar images digitally every 30 seconds. Combined radar images from the two vessels (each radar image was about 11.1 km in diameter) covered the receiver and about two thirds of the acoustic track. Mm.1 shows a movie of the ships' radar images following the ISW during this event, from 18:00 GMT on 17 August to 02:00 GMT on 18 August, 2006. In this paper we discuss two situations when the ISW packet had not reached the acoustic track at time period Tg_1 (20:30 to 20:37 GMT) and when the ISW occupied most of the acoustic track at time period Tg_2 (22:00 to 22:07 GMT). The radar images from both vessels at 20:30 GMT and 22:00 GMT are shown in Figs. 2(a) and 2(b) respectively.

At 20:30 GMT, the R/V Sharp radar showed 10 distinct ISW fronts in a packet. At the same time, the R/V Oceanus radar showed 7 wave fronts with less curvature. The spacing between wave fronts in the packet varied from ~ 0.4 to 0.5 km for the leading wave fronts to ~ 0.2 to 0.3 km for the trailing waves. The ISW direction of propagation was about compass direction 305^o.

At 22:00 GMT, most of the acoustic track including the receiver array was occupied by the ISW packet [see Fig. 2(b)]. The physical characteristics of the ISW packet during this time were similar to those at 20:30 GMT, except that its propagation direction was slightly changed. The R/V Oceanus observed, close to the receiver, the ISW propagation direction to be about 320^o. At the middle of the acoustic track (SW20), the propagation direction was 310^o observed on RV Sharp. Thus the angle between the ISW fronts and the acoustic track at midpoint was about 10^o. The average speed of the ships following the ISW packet was about 1.8 to 2.0 knots, which is similar to the ISW propagation speed. Note that the wave front was curved so there is a natural discrepancy between the propagation directions observed by two ships.

The SW45 mooring had eleven temperature sensors located between 15 m to 72 m and the SW54 mooring had ten temperature sensors at 13.25 m to 78.5 m. To get a spatial picture of the water temperature along the acoustic track, data from a third thermistor string (SW20) in the middle of the track is also used. This mooring had only three temperature sensors at 21 m to 45 m. All these sensors recorded the temperature data every 30 seconds.

Fig. 3 shows the temperature records at the receiver mooring SW54, midpoint SW20, and acoustic source SW45 from 20:00 to 23:00 GMT on August 17, 2006. A solitary internal wave arrived at the receiver around 21:15 GMT, followed by a calm period of about one hour. At around 21:40 GMT, the leading front of a strong ISW packet passed the receiver position. The ISW packet caused a sudden increase in the thermocline depth. At 22:20 GMT, the water temperature decreased slowly until 09:00 GMT the next day. The leading wave front was observed at SW20 at 22:01 and SW45 at 22:15 GMT respectively. If we assume the leading wave front is linear (it is not) and the wave speed is constant along the wave front, this suggests an angle of about 5^o between the advancing front and the acoustic track.

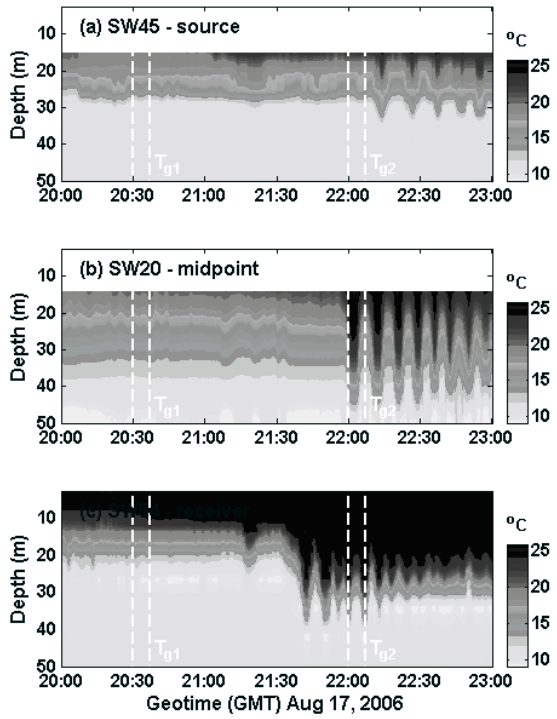

Fig. 3 Temperature profiles measured at (a) acoustic source, (b) the midpoint between the source and receiver, and (c) at the Shark WVHLA during internal wave Event 50, August 17, 2006 from 20:00 to 23:00 GMT.

Next, we show the acoustic signal arrival on the Shark VHLA during the two periods Tg_1 and Tg_2. In order to show the intensity variations, we show the arrival of two different LFM pings on the array at geotimes separated by 102 sec. In Fig. 4(a), the upper panel shows the acoustic signal on the VLA at 20:30:15 GMT while the lower panel shows the same signal arriving on the HLA.

Figure 4(b) shows the same two arrays at 20:31:57 GMT. The parallel lines on the HLA data shown in the lower panel are due to the interference of horizontal ray mode arrivals. The data on the VLA portion of the array shown in the upper panel best represent the modal arrivals. Note the similarity of the intensity values on both vertical and the horizontal array plots in Figs. 4(a) and (b), indicating the stability of the arriving signal energy during Tg_1.

At Tg_2 the same data format is shown. At 22:04:55 GMT shown in Fig. 4(c), both the VLA and HLA show drastic change in the arrival. The signal intensity becomes very strong; however, different modal and ray arrivals are mixed together and difficult to separate. At 22:06:35 GMT shown in Fig. 4(d), the modal and ray arrivals show a lack of structure as well as lower intensity. During the time period of Tg_2, the ISW is occupying a large fraction of the acoustic track. To further quantify these results, we next calculate the averaged intensity in geotime and depth for the periods, Tg_1 and Tg_2.

3 Intensity variations

Based on the theory proposed in our previous work[3], the angle between the ISW fronts and the acoustic track determines the mechanism of the intensity fluctuations. Small angles provide horizontal refraction and focusing while larger angles cause mode coupling. In between these limits, there is an angular region for which the propagation is adiabatic. During internal wave Event 50, the ISW fronts passed through the acoustic track at an angle of about 5^o providing the condition for horizontal refraction. Prior to the ISW arrival, we observe stable adiabatic propagation in a stable water column. Hence, a transition can indeed be observed between these two mechanisms.

To show a focusing event, we consider two geotimes: (a) Tg_1 when the leading internal wave front had not reached the acoustic track and, (b) Tg_2 when the internal wave

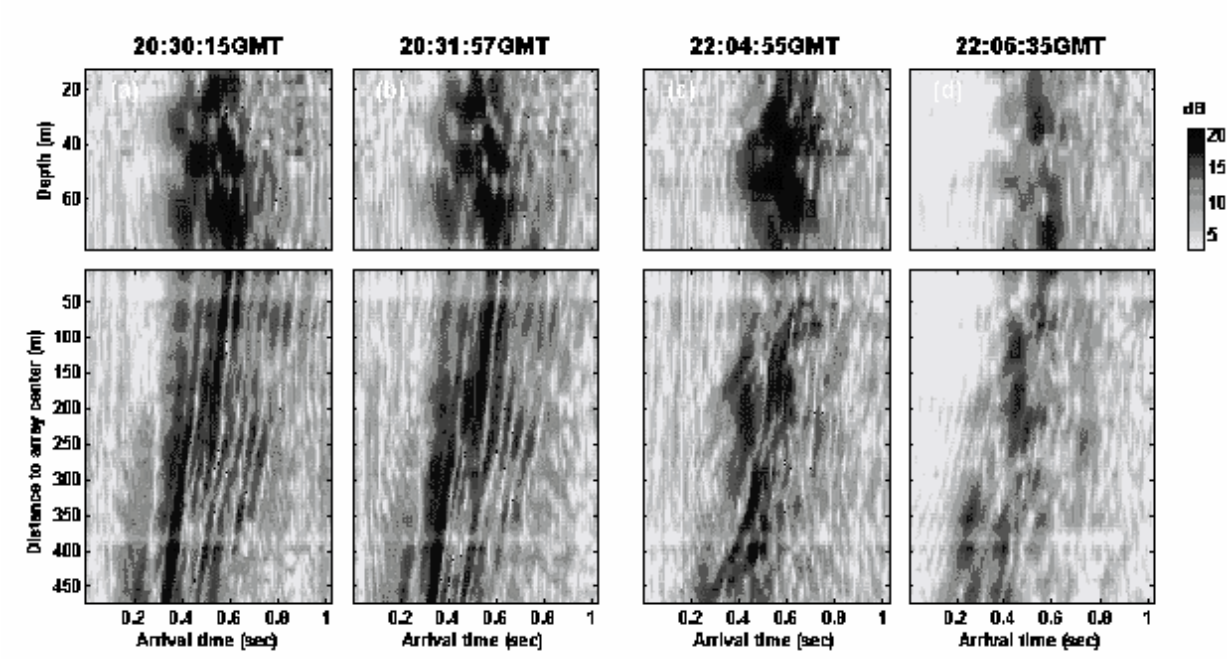

Fig. 4 Received acoustic intensity on the Shark VHLA during two geotimes within the Tg_1 and Tg_2 periods. Upper panel shows the acoustic field on the VLA portion of the array while the lower panel shows the HLA portion. (a) Tg = 20:30:15 GMT, (b) Tg = 20:31:57 GMT, (c) Tg = 22:03:39 GMT, (d) Tg = 22:05:21 GMT.

packet occupied most of the acoustic track. We calculate the total intensity integrated over the depth *H* as

$$I(T) = \int_0^H I(z,T)dz \qquad (1)$$

where $I(z,T) = \frac{1}{\rho c}\int_{\tau}^{\tau+\Delta\tau} p^2(z,T,t)dt$ is the intensity of the signals integrated over a pulse length $\Delta\tau$ at a given depth z, *p* is acoustic pressure, ρ is the water density, and *c* is the sound speed. The distribution of the ISW's in the horizontal plane can be assessed by carefully examining the radar image and the depth distribution of the temperature at three points (SW45, SW20, SW54) along the acoustic track.

The temperature distribution starting at 20:30:00 GMT (Tg_1) for the transmission period (i.e. ~ 7.5 minutes) at three different moorings shows very little fluctuation along the acoustic track (see Fig. 2). This indicates that the ISW has not reached the acoustic track during Tg_1, as is also shown in the radar image. In Fig. 5(a) we show a plot of *I(z,T)* for the VLA. It is shown that for a repeated pulse of the same radiated intensity, very small intensity variations exist. In Fig. 5(b) we plot the depth integrated intensity for all geotimes, *I(T)*. The very small fluctuations (~ 3 dB) at Tg_1 indicate a quiescent condition without ISW's in the track. This means that during this period of observation there is no redistribution of sound energy in the horizontal plane, or there is no horizontal refraction. Small variations of the depth distribution of the sound intensity correspond to the adiabatic case. Figure 5(c) shows the acoustic intensity on the HLA. There are no apparent intensity variations on the HLA during this geotime.

Similar to Fig. 5(a), *I(z,T)* for Tg_2 is plotted in Fig. 5(d). Here we see increasing and decreasing trends in sound intensity over the VLA, synchronous in depth. The value of calculated averaged intensity *I(T)* using Eq. (1) peaks to ~ 35 dB around 22:04:30 to 22:05:00 GMT, and decreases to ~ 20 dB around 22:06:35 GMT as shown in Fig. 5(e). This significant fluctuation corresponds to redistribution of the acoustic energy in the horizontal plane, which in the limit can be referred to as focusing or defocusing events and is related to the position of the source and/or receiver with respect to the internal wave crests. The focusing and defocusing are also shown in Figs. 4(c) and 4(d). In this case (i.e. Tg_2), the receiver is between two adjacent maxima of the thermocline displacement, and the high intensity fluctuations (~ 15 dB peak to peak) are due to the horizontal refraction effects similar to those shown in the previous studies[3]. Temporal fluctuations correlate with the oscillations of the thermocline layer at the receiver (see Fig. 3) due to ISW's (period is ~ 6-8 min). The fluctuations in the presence of internal waves (i.e. at Tg_2) are about 15 dB, which are much larger than those of Tg_1 (~ 3 dB) with no internal wave in the acoustic track. Although the total jump in the thermocline thickness (i.e. from ~ 15 m to ~ 30 m) could make a difference in the 'absolute' value of the acoustic intensity, it does not play a big role in inducing the temporal intensity fluctuation with the periods corresponding to the ISW.

As in the quiescent case shown above, Fig. 5(f) shows the acoustic intensity on the HLA for this active period. During the geotime of about 7.33 minutes, we see the variation of the sound field at the horizontal array. For the variation observed during the first 3 minutes, there are two large intensity maxima observed at the HLA. These become weaker and disappear during the second half of the time period (after 22:03). This behavior, in our opinion, is a manifestation of horizontal refraction. The sloped intensity modulations correspond to the motion of an interference pattern registered on the horizontal array, which can be result from any motion of the water layer (such as an ISW packet). The velocity of this interference pattern is estimated as 1–1.5 m/s from the acoustic data [shown as a slope in Fig. 5(f)]. This may not be directly related with the velocity of the internal solitons (measured from shipboard radar to be about 1 m/s). Further detailed modeling is needed to understand the nature of these fluctuations and their relationship to the slope of the lines shown in Fig. 5(f).

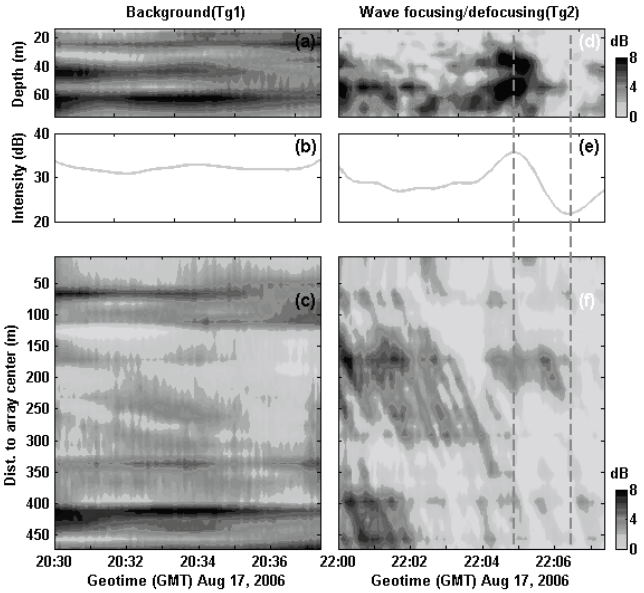

Fig. 5 Received acoustic intensity during a 440 sec (~ 7.33 mins) transmission period for two geotimes, Tg_1 (from 20:30:00 to 20:37:30 GMT): (a) depth distribution of total intensity per pulse I(z,T), (b) depth integrated intensity, I(T) for VLA, (c) total intensity I(x,T) for HLA; and Tg_2 (22:00:00 to 22:07:30 GMT): (d) depth distribution of total intensity per pulse I(z,T), (e) depth integrated intensity, I(T) for VLA, (f) total intensity I(x,T) for HLA.

Summary

SW06 experiment has provided high quality acoustic and environmental data to investigate the acoustic wave interaction with internal waves. Preliminary analysis of acoustic data and observations of radar images and temperature records show that during the passage of an ISW event, the underlying mechanism of significant acoustic intensity variation is horizontal refraction. This observation agrees with the recently proposed theory of sound propagation through ISW[3]. Future work includes mode and frequency filtering of this acoustic data as well as modeling to establish the transition of acoustic field from adiabatic to other mechanisms when an ISW passes an acoustic track.

Acknowledgments

The authors wish to thank all participants of the SW06 experiment, especially the scientific and ship personnel aboard the R/V Sharp and R/V Oceanus. This research was supported by the Ocean Acoustic Program (321OA) of the Office of Naval Research through Grant [N00014-07-1-0546].

References

[1] Badiey, M., Y. Mu, J. Lynch, J. R. Apel, and S.Wolf, "Temporal and azimuthal dependence of sound propagation in shallow water with internal waves," IEEE J. Oceanic Eng. 27(1), 117-129 (2002).

[2] Badiey, M., B. G. Katsnelson, J. F. Lynch, S. Pereselkov, and W. L. Siegmann, "Measurement and modeling of three-dimensional sound intensity variations due to shallow-water internal waves," J. Acoust. Soc. Am. 117(2), 613-625 (2005).

[3] Badiey, M., B. G. Katsnelson, J. F. Lynch, and S. Pereselkov, "Frequency dependence and intensity fluctuations due to shallow water internal waves," J. Acoust. Soc. Am. 122(2), 747-760 (2007).

[4] Collis, J. M., T. F. Duda, J. F. Lynch, H. A. DeFerrari, "Observed limiting cases of horizontal field coherence and array performance in a time-varying internal wavefield," JASA, this issue (2008).

[5] Lin, Y-T, J. F. Lynch, T. F. Duda., A. E. Newhall, "Investigation of three dimensional sound propagation in shallow water regions," JASA, this issue (2008).

[6] Newhall, A. E., T. F. Duda, J. D. I. K. von der Heydt, J. N. Kemp, S. A. Lerner, S. P. Liberatore, Y.-T. Lin, J. F. Lynch, A. R. Maffei, A. K. Morozov, A. Shmelev, C. J. Sellers, and W. E. Witzell, "Acoustic and oceanographic observations and configuration information for the WHOI moorings for the SW06 experiment," WHOI technical report #WHOI-2007-04, (2007).